

Measurement and analysis of the Hall effect of A-Fe₂As₂ single crystals with A = Ba, Ca or Sr.

C. L. Zentile, J. Gillett, S. E. Sebastian, and J. R. Cooper

Cavendish Laboratory, University of Cambridge, J. J. Thomson Avenue, Cambridge, CB3 0HE, United Kingdom

(Dated: July 20, 2021)

We report measurements of the Hall coefficient R_H for single crystals of AFe₂As₂ with $A = Ba, Ca$ or Sr which are the anti-ferromagnetic parent compounds of some high temperature pnictide superconductors. We show that R_H of Sr-122 is consistent with high field quantum oscillation data. Our $R_H(T)$ data can also be used to estimate values of the spin density wave gap, giving $\Delta_{SDW}(0) = 710 \pm 70$ K for Sr-122 and 435 ± 20 K for Ba-122.

PACS numbers: Valid PACS appear here

The discovery of high temperature superconductivity in the iron pnictides has generated considerable scientific interest. They are correlated electron systems with quasi-2D structure, and show both similarities with, and notable differences from, the cuprates. Here we report measurements of the Hall coefficient R_H for three isostructural ‘122’ iron arsenides that all have a structural phase transition at a temperature T_S . It is believed [1, 2, 3] that anti-ferromagnetic (AF) order also sets in at T_S , and that superconductivity occurs when this is suppressed by doping with K [4], Na or Co or by applying pressure [5].

Fig. 1 shows the in-plane resistivity $\rho(T)$ versus T for three of the crystals for which R_H was measured just over a year ago. While their resistivity ratios (RR) summarized in Table I are slightly lower than published values [6, 7, 8, 9], higher values have since been obtained [10] and Sr crystals from similar growth batches were used for quantum oscillation (QO) experiments [11]. Also our Hall mobility ratios $\mu_H(T \rightarrow 0)/\mu_H(300) \approx 200$ are substantially higher than the RR values. Further evidence for sample quality is the sharpness of the phase transitions shown by the derivative plots $d\rho/dT$ in the inset to Fig. 1. The T_S values in Table I, defined by the maxima in $|d\rho/dT|$ for Sr and Ca and from the temperature of the step increase in $d\rho/dT$ for Ba, agree well with published data [6, 7, 8, 9]. Above T_S , $\rho(T)$ for the Ba and Sr crystals shows upward deviations from linearity as indicated by the faint lines in Fig. 1 and by the fall in $d\rho/dT$ shown in the inset. This could arise from the onset of magnetic or structural fluctuations ~ 40 K above T_S . In contrast, Ca-122 shows a slight downward deviation from linearity above T_S . Below $T_S/2$ the $\rho(T)$ curves vary as $A + BT$ over a considerable range of T . For Sr-122 this is followed by a slight upturn below 30 K reminiscent of the Kondo effect while for Ca-122 $\rho(T)$ flattens out as T^3 below 30 K. Unusually, $\rho(T)$ for Ba-122 falls linearly to the lowest measured temperature of 5 K.

Hall effect measurements were made on crystals of Ca-122 and Sr-122, from two growth batches, all grown using Sn flux. These long, thin bars were $1.7 - 0.5 \times 0.6 - 0.3 \times 0.1 - 0.05$ mm³ in size and had two pairs of Hall contacts that were measured simultaneously to check for uniformity and reproducibility. The Van der

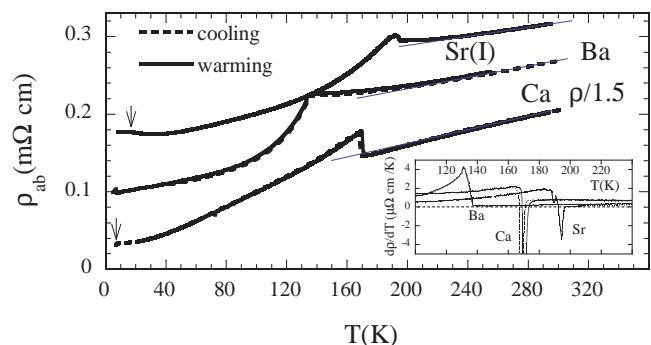


FIG. 1: Zero-field resistivity as a function of T , $\rho(T)$ for single crystals of AFe₂As₂ ($A = Ba, Ca, Sr$). The arrows show changes in slope arising from a small amount of parasitic superconductivity [12, 13]. The inset shows $d\rho/dT$ near the phase transitions.

Pauw four-contact method was used for a thin flake of Ba-122, $1.2 \times 1.2 \times 0.02$ mm³ in size, grown using self-flux. The magnetic field was directed along the c -axis and was repeatedly reversed by rotating the sample stage by 180°. Our $R_H(T)$ curves in Fig. 2 show remarkably similar shapes, signs and magnitudes for the four samples. R_H increases approximately linearly by a factor of 3 between 20 and 60-80 K followed by notable flattening well below T_S . This flattening could be associated with the proposed spin density wave (SDW) state. Below 120 K R_H is negative for all the samples but for Ca-122 and the higher purity Sr(I) crystal there is a region between $T_S - 40$ and T_S where $R_H > 0$, suggesting a different balance between electron and hole contributions there. Above T_S , $|R_H|$ for Ca-122 rises slightly and then becomes constant. The other two compounds show a linear increase in $|R_H|$ between 300 K and T_S^+ .

Three QO studies of in AFe₂As₂ in magnetic fields as high as 55 T have been reported [11, 14, 15] and the results analyzed in terms of small ellipsoidal pockets. We find that our Hall data are consistent with the QO results, especially for Sr-122. *A priori* they could be very different because there is an even number of electrons per unit cell in both the high- T tetragonal phase and the low- T phase where there is a commensurate anti-ferromagnetic

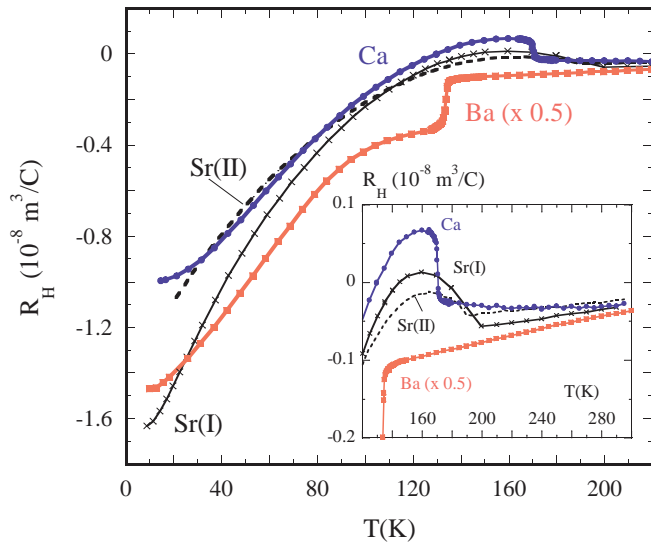


FIG. 2: Color online: T dependence of the Hall coefficient, $R_H(T)$ for single crystals of AFe_2As_2 ($A = \text{Ba}, \text{Ca}, \text{Sr}$) with a field of $5 \text{ T} \parallel c$. The inset shows the transitions and high- T region on an expanded scale.

(AF) wave vector [1, 2, 3] that halves the in-plane Brillouin zone area. In both cases the number densities of electrons (n_e) and holes (n_h) will be the same and their contributions to R_H should be weighted by the corresponding electrical conductivities σ , e.g. for two bands:

$$R_H = \frac{|R_H^h|\sigma_h^2 - |R_H^e|\sigma_e^2}{(\sigma_e + \sigma_h)^2} \quad (1)$$

So if n_h and n_e are the same, and $\sigma_h \simeq \sigma_e$, R_H can be very small indeed, and will not give a valid measure of the carrier concentration. It might well vary strongly from sample to sample depending on the precise balance between e and h contributions. We see from Table I that there is actually good agreement between our values of $R_H(10 \text{ K})$ and those in the literature despite the differences in the RR values mentioned earlier. Another possible source of discrepancies between high field QO and lower field Hall effect work is magnetic breakdown (MB) [16]. In a weak-coupling SDW system, the energy gap (Δ_{SDW}) is small [17]; $\Delta_{SDW} = 1.76k_B T_S$ since the gap equation for an SDW has the same form as in BCS superconductivity. In practice, and perhaps surprisingly, any MB effects seem to be small.

For a single ellipsoidal pocket, the standard, nearly free electron formulae $R_H = 1/ne$ and $\sigma_i = ne^2\tau/m_i$ are still valid [18]. Here m_i is the effective mass along a principal axis (i) of the ellipsoid, and $n = 2V_k/(2\pi)^3$, where V_k is its volume in k -space. For Sr-122 three pockets labelled α , β and γ were detected [11] with frequencies of 370 ± 20 , 140 ± 20 and $70 \pm 20 \text{ T}$ and in-plane k space areas of 1.38, 0.52 and 0.26% of the paramagnetic Brillouin zone area, $(2\pi/a)^2$, where the in-plane lattice pa-

rameter [1, 9] $a = 3.93 \text{ \AA}$. Angular studies showed that the ellipsoids were elongated along the crystallographic c -axis with axis ratios (r) of 1.4, 6.1 and 3.3 for α , β and γ respectively. Later three similar frequencies and smaller m^* values were found for Ba-122 crystals [14]. Band-structure calculations [11, 14] predict 4 inequivalent pockets in the AF Brillouin zone arising from imperfect nesting of the AF vector $\vec{Q} = (\frac{\pi}{a}, \frac{\pi}{a}, 0)$. As discussed below, analysis of the Hall data suggests that the largest electron pockets are absent for Sr-122.

From the values of r and the k space areas we obtain V_k for each type of ellipsoidal pocket. Each pocket in the reduced AF Brillouin zone gives $n_\alpha = 0.0053(5)$, $n_\beta = -0.0054$ and $n_\gamma = -0.001(0)$ carriers per formula unit ($f.u.$). Here the + and - signs denote h and e contributions to R_H respectively. Within the error bars these satisfy $\Sigma n_e = \Sigma n_h$ and imposing this as a precise constraint does not affect our conclusions. Both papers [11, 14] identify α as a “tear-shaped” hole pocket, and β as an ellipsoidal electron pocket. The small γ pocket is identified as electron-like for Sr-122 in Ref. 11 and as hole-like for Ba-122 in Ref. 14. Using the analysis described below we get good agreement with our Hall data if the γ pocket is electron-like for Sr-122.

In order to calculate R_H we need to find appropriate values of σ_α , σ_β and σ_γ for use in Eqn. 1. Experimentally [19] it was found that the isotropic mean free path approximation worked well for Sr_2RuO_4 . Here we are dealing with small values of k_F but any impurity potentials will still be screened over short distances (d) because of the underlying metallic state that is weakly perturbed by a SDW. In this limit, $k_F d \ll 1$ we expect a k -independent scattering cross-section, $4\pi d^2$ [20], which will indeed give a mean free path that is independent of k . The relative contributions to σ in Eqn. 1 are then given by n_α/k_F^α etc. where k_F^α is the in-plane Fermi wave-vector of the α pocket and give a negative value for R_H .

Band-structure calculations [11, 14] seem to give two pockets of each type in the AF Brillouin zone. Taking this into account leads to an effective electron concentration $n_{eff} = 0.039$ per $f.u.$. This is in excellent agreement with the value given in Table I for Sr-122 for a field of 5 T at low T . Although $\Sigma n_e = \Sigma n_h$ within error bars, there is little $e - h$ cancellation in R_H because the α and β pockets have very different eccentricities r , which means that $\sigma_\alpha \neq \sigma_\beta$. If instead we included the fourth and largest electron pocket in this analysis, using the eccentricity implied by the band-structure calculations, then the calculated value of $n_{eff} = 0.11$ per $f.u.$, which is much larger than the experimentally determined values.

The above analysis has all been based on R_H data taken at 5 T . As shown in Fig. 3 R_H is in fact field-dependent. We do not understand this, but although the three materials show completely different H -dependences, it could still be a general property of the SDW state because of the $e - h$ compensation described above. For the Sr-122 crystal R_H increases by nearly 50% be-

TABLE I: Parameters obtained in the present work or used in the analysis. T_S values were obtained on cooling; for $A = Ca$ the warming transition is 2K higher. RR is the resistivity ratio $\rho(300)/\rho(10)$. R_H is the Hall coefficient measured at 5 T, n_{eff} is the corresponding carrier concentration in a single band analysis. μ_H is the Hall mobility, $R_H\sigma$, and β is the T^2 coefficient of the inverse mobility obtained from fits to $1/\mu_H = \alpha + \beta T^2$ between 10 and 60 K. Sr(I) is from growth batch 170 and Sr(II) batch 105.

	Ba	Ca	Sr(I)	Sr(II)
$V_{f.u.}(\text{\AA}^3)$	102	89	95	95
T_S (K)	135.4	168.6	194.6	190.8
RR	2.65	6.2	1.85	1.5
RR (other work)	(4.3) ^a	(11) ^b	(4.7) ^c	-
$R_H(295)(10^{-10}\text{m}^3/\text{C})$	-7.6	-3.0	-3.0	-2.3
$R_H(T_S+5)(10^{-10}\text{m}^3/\text{C})$	-21.0	-2.5	-5.5	-4.1
$R_H(10)(10^{-10}\text{m}^3/\text{C})$	-292	-99	-162	-120
$R_H(10)(10^{-10}\text{m}^3/\text{C})$	(-220) ^a	(-95) ^b	(-135) ^c	-
$n_{eff}(10)/\text{f.u.}$	0.022	0.056	0.037	0.049
$\mu_H(295)(\text{cm}^2/\text{Vs})$	2.8	0.98	0.95	-
$\mu_H(T_S + 5)(\text{cm}^2/\text{Vs})$	9.3	1.3	1.9	-
$\mu_H(0)(\text{cm}^2/\text{Vs at 1T})$	450	200	200	50
$\beta(1\text{T})(10^{-6}\text{Vs}/\text{cm}^2/\text{K}^2)$	0.8	2.9	-	5.3
$\beta(5\text{T})(10^{-6}\text{Vs}/\text{cm}^2/\text{K}^2)$	0.9	3.3	4.1	5.1

^a Ref. 6, ^b Ref. 9, ^c Refs. 7, 8

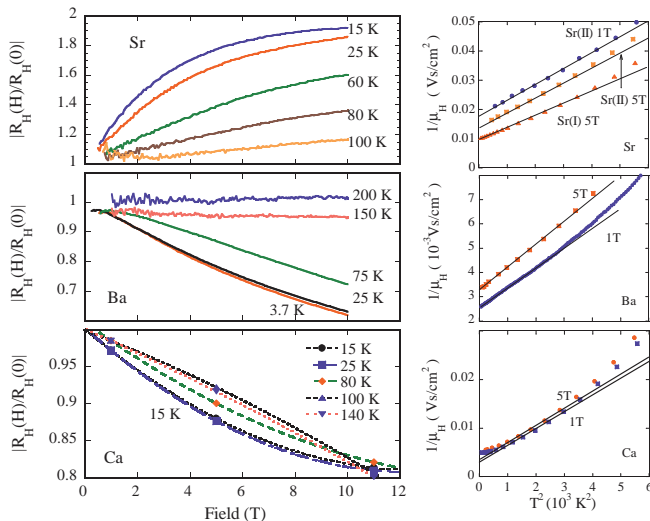


FIG. 3: Color online: left-hand panels, normalized magnetic field dependence of the measured Hall coefficient $|R_H|$ for the three compounds studied here, at several fixed T . Right hand panels, inverse Hall mobility $vs.$ T^2 for the 3 compounds studied.

tween 1 and 5 T. In principle this could be caused by one or more of the pockets approaching the usual high field condition, $\mu_H H$, i.e. $\omega_c \tau \sim 1$ at 5 T. But for the same crystals we did not observe any QOs in fields from 12 to 15 T down to 1.4 K. Therefore any explanation along these lines seems to require a very small pocket of frequency ≈ 50 T or less whose period was too long to be

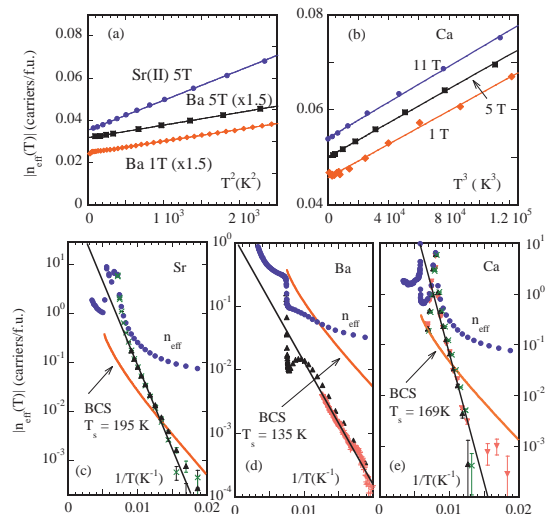


FIG. 4: Color online: (a) plots of effective carrier concentration n_{eff} $vs.$ T^2 for Sr-122 and Ba-122. The lines show the fits to $C + DT^2$. (b) n_{eff} $vs.$ T^3 for Ca-122 and the corresponding fits for three values of applied magnetic field (T). (c) - (e) semi-log plots $n_{eff}(T)$ $vs.$ $1/T$ before and after subtraction of the limiting low T dependence. For Sr and Ba, black triangles show data at 5 T while crosses show data at 1 T. For Ca black triangles, inverted triangles and crosses show 5 T, 1 T and 11 T data respectively. The thicker, slightly curved, (red) lines show calculated weak-coupling BCS behavior for the T_S values shown. The slopes of the black lines are used to find the activation energy, i.e. $\Delta_{SDW}(0)$.

observed in our measurements. For Ca-122 the H dependence is much smaller and of opposite sign, while that for Ba-122 is larger and also has the opposite sign to that in Sr-122. High field orbital effects are somewhat more likely here because Ba-122 has a higher average mobility and our Ca-122 crystal has comparable mobility to the Sr crystal but shows a much smaller H -dependence.

Applying the same analysis to available data for Ba-122 [14] does not give such straightforward results. If the largest e -pocket is again absent [14], we can satisfy $\Sigma n_e = \Sigma n_h$ and account for the *low field* value of R_H by assuming that the β pocket has $r = 3$, rather than 5 ± 1 [14], that γ is in fact an e -pocket and by assuming that the mean free path on the β and γ electron pockets is 20% larger than that on the α pockets. For Ca-122 [15], the two pockets observed have very different volumes so we have not attempted to calculate R_H .

Fig. 3 also shows that the inverse Hall mobility of all crystals studied obeys an $\alpha + \beta T^2$ law, although the range of this fit is very small for Ca-122 and actually a T^3 law gives a better fit. For the cuprate superconductors its presence over a wide range of hole doping with little change in β is an important empirical observation. In the present case, as for Co-doped crystals [6] it seems to arise from $e - h$ pockets whose E_F values are extremely low. From the QO data we find E_F equals 240, 120 and 100 K for the α, β and γ [21] pockets in Sr-122 and 490,

403 and 115 K for Ba-122. As shown in Table I the βT^2 term in $1/\mu_H(T)$ is a factor 4 larger for Sr-122, reflecting the smaller E_F values listed above.

We now address the T dependence of R_H at low T and propose a method of estimating the SDW gap from our data. An important clue here is that for Ba-122 the electronic heat capacity above T_S is ~ 8 times larger than the low T value [22]. This suggests that, although the small pockets do give a finite density of states (DOS) at E_F , any square-root singularities in the DOS from the SDW will be much larger. As shown in Fig. 4a, for Sr-122 and Ba-122 we can fit $n_{eff}(T)$ below 40-50 K to a $C + DT^2$ law. This DT^2 term could arise partly from the low values of E_F combined with the constraint $\Sigma n_e = \Sigma n_h$, leading to changes in n_e or n_h as T is increased. A second possible reason is that in Eqn. 1, $\sigma_{\alpha,\beta,\gamma}$ could have different T^2 terms from $e - e$ scattering; a third is that the pockets expand as the SDW gap decreases. While the latter must be true at higher T , in Fig. 4 we also show n_{eff} vs. $1/T$ plots calculated [25] for the fully nested case where there are no pockets and the energy gap $2\Delta_{SDW}(T)$ has the usual BCS s -wave T -dependence. These plots are linear below $T_{SDW}/2$ implying that Δ_{SDW} is effectively constant and any expansion of the pockets is not important below $T_{SDW}/2$. As shown in Fig. 4, subtraction of the $C + DT^2$ terms leads to linear regions in plots of $\log n_{eff}$ vs. $1/T$. From the slopes of these lines we find $\Delta_{SDW}(0) = 710 \pm 70$ K for Sr-122, a factor of 2.1 larger than the BCS value, and 435 ± 20 K for Ba-122, a factor of 1.8 larger than BCS. For Ca-122 the value of $\Delta_{SDW}(0)$ is less certain. As shown in Fig. 4b, $n_{eff} =$

$C + DT^3$ gives a good fit below 50 K. Subtracting this gives $\Delta_{SDW}(0) = 1150 \pm 150$ K, a factor 3.9 larger than BCS. On the other hand if n_{eff} is forced to fit $C + DT^2$ at low T , then a much smaller value of $\Delta_{SDW}(0) \sim 1.2$ times the BCS value, is obtained.

Single crystal optical reflectivity data taken at 10 K have been analyzed in terms of two broad Lorentz-Drude peaks centered at 360 and 890 cm^{-1} for Ba-122 [23, 24] and at 500 and 1360 cm^{-1} for Sr-122 [23]. The lower peaks have similar energies to our values, $\Delta_{SDW}(0) = 300 \pm 15$ cm^{-1} for Ba-122 and 490 ± 50 cm^{-1} for Sr-122. Moreover, there are clear changes in slope in the raw reflectivity data [23] at *ca.* 270 and 600 cm^{-1} for Ba-122 and at 410 and 900 cm^{-1} for Sr-122 that are absent above T_S . We therefore suggest that the lower reflectivity anomaly could correspond to the onset of electron excitations between the $e - h$ pockets at E_F and the square root singularities from the SDW at $E_F \pm \Delta_{SDW}$ which would have an energy of $\Delta_{SDW}(0)$, while the upper anomaly could be a measure of $2\Delta_{SDW}(0)$.

In summary, our Hall measurements on Sr-122 are surprisingly consistent with high-field quantum oscillation data, and subject to some minor modifications, with those observed for Ba-122. We have been able to make approximate estimates of the SDW gaps from the Hall data. For Sr and Ba we propose that these are consistent with optical reflectivity although detailed calculations of the latter are still needed.

We are grateful to S. Battacharya, T.M. Benseman, A. Carrington, J.W. Loram, and J.G. Storey for helpful discussions and to the EPSRC (U.K.) for financial support.

-
- [1] J. Zhao, W. Ratcliff, J.W. Lynn, G.F. Chen, J.L. Luo, N.L. Wang, J. Hu, and P. Dai. Phys. Rev. B **78**, 140504(R) (2008).
- [2] Q. Huang, Y. Qiu, W. Bao, M.A. Green, J.W. Lynn, Y.C. Gasparovic, T. Wu, G. Wu, and X.H. Chen. Phys. Rev. Lett. **101**, 257003 (2008).
- [3] A.I. Goldman, D.N. Argyriou, B. Ouladdiaf, T. Chatterji, A. Kreyssig, S. Nandi, N. Ni, S.L. Budko, P.C. Canfield, and R.J. McQueeney. Phys. Rev. B **78**, 100506(R) (2008).
- [4] M. Rotter, M. Tegel and D. Johrendt. Phys. Rev. Lett. **101**, 107006 (2008).
- [5] P.L. Alireza, Y.T.C. Ko, J. Gillett, C.M. Petrone, J.M. Cole, G.G. Lonzarich and S.E. Sebastian, J. Phys.: Condens. Matter **21**, 012208 (2009).
- [6] F. Rullier-Albenque, D. Colson, A. Forget, and H. Alloul. Phys. Rev. Lett. **103**, 057001 (2009).
- [7] G.F. Chen, Z. Li, J. Dong, G. Li, W.Z. Hu, X.D. Zhang, X.H. Song, P. Zheng, N.L. Wang, and J.L. Luo. Phys. Rev. B **78**, 224512 (2008).
- [8] J.Q. Yan, A. Kreyssig, S. Nandi, N. Ni, S.L. Budko, A. Kracher, R.J. McQueeney, R.W. McCallum, T.A. Lograsso, A.I. Goldman, and P.C. Canfield. Phys. Rev. B **78**, 024516 (2008).
- [9] F. Ronning, T. Klimczuk, E.D. Bauer, H. Volz, and J.D. Thompson. J. Phys.: Condens. Matter **20**, 322201 (2008).
- [10] P. Syers, J. Gillett, A. Ming, and S.E. Sebastian. (2009) unpublished.
- [11] S.E. Sebastian, J. Gillett, N. Harrison, P.H.C. Lau, D.J. Singh, C.H. Mielke, and G.G. Lonzarich. J. Phys.: Condens. Matter **20**, 422203 (2008).
- [12] S.R. Saha, N.P. Butch, K. Kirshenbaum, J. Paglione, and P.Y. Zavalij. Phys. Rev. Lett. **103**, 037005 (2009).
- [13] H. Hiramatsu, T. Katase, T. Kamiya, M. Hirano, and H. Hosono. Phys. Rev. B **80**, 052501 (2009).
- [14] J.G. Analytis, R.D. McDonald, J.-H. Chu, S.C. Riggs, A.F. Bangura, C. Kucharczyk, M. Johannes, and I.R. Fisher. Phys. Rev. B **80**, 064507 (2009).
- [15] N. Harrison, R.D. McDonald, C.H. Mielke, E.D. Bauer, F. Ronning, and J.D. Thompson. J. Phys.: Condens. Matter **21**, 322202 (2009).
- [16] D. Shoenberg, "Magnetic oscillations in metals", Cambridge University Press, Cambridge, U.K. (1984).
- [17] G. Grüner "Density Waves in Solids", Frontiers in Physics vol.89 (1994).
- [18] N.F. Mott and H. Jones, "The theory of the properties of metals and alloys", Oxford University Press, Oxford, U.K. (1936).
- [19] A.P. Mackenzie, N.E. Hussey, A.J. Diver, S.R. Julian, Y. Maeno, S. Nishizaki, and T. Fujita, Phys. Rev. B **54**, 7425 (1996).

- [20] L.I. Schiff, Chapter V “Quantum Mechanics”, McGraw-Hill, New York, (1955).
- [21] We took m^* data for α and β from Ref. 11 and $m^* = 0.9m_e$ for the γ pocket from Ref. 26.
- [22] J.G. Storey, J.W. Loram, J.R. Cooper, Z. Bukowski and J. Karpinski, preprint (Sept. 2009).
- [23] W.Z. Hu, J. Dong, G. Li, Z. Li, P. Zheng, G.F. Chen, J.L. Luo, and N.L. Wang. Phys. Rev. Lett. **101**, 257005 (2008).
- [24] F. Pfunder, J.G. Analytis, J.-H. Chu, I.R. Fisher, and L. Degiorgi, Eur. Phys. J. B **67**, 513 (2009).
- [25] Here n_{eff} is the number of electrons excited above the gap. There will be an equal number of holes below the gap, but usually enough $e-h$ asymmetry to give $n_{eff} \sim \exp(-\Delta/T)$.
- [26] N. Harrison and S.E. Sebastian
<http://arxiv.org/abs/0910.4199v1>.